VERIFICATION OF RadCAD: SPECULAR CAPABILITIES

S1-61
056791

Sam Lucas
Cullimore and Ring Technologies
Littleton, CO

Abstract

As part of the RadCAD's development process, it is necessary to compare RadCAD's results with other radiation tools and exact solutions when and where possible. Form factor algorithms have been previously verified with exact solutions. This paper will consider RadCAD's specular capabilities. First, radiation exchange factors will be compared against exact solutions and results from TRASYS for various geometries. Critical dimensions and optical properties are changed for each geometry. Second, a specular adjunct plate system will be used to verify absorbed heat fluxes. This particular geometric problem has had some attention in the literature. Previous authors have used this problem to validate software results with exact analytical solution. This paper will compare absorbed heat rates against the exact solution and other published results from other thermal radiation tools.

The agreement between RadCAD and the exact solutions is good. The maximum error for both specular and diffuse exchange factors for both geometries and all optical properties was 3%. The absorbed fluxes differed by a maximum of 4% for the adjunct plate problem.

Nomenclature

A	surface area	(m^2)
E	percent error	(-)
L	length	(m)
N_r	number of rays shot per surface	(-)
$Q_{e/ab}$	radiant energy rate leaving the cavity	(W)
$(Q_{e/ab})_b$	radiant energy rate leaving a black cavity	(W)
R	radius	(m^2)
R_A	result from an analytical solution	(W,-)
R_S	result from a simulation tool	(W,-)
α	absorptivity	(-)
$\bar{\varepsilon}$	radiating effectiveness	(-)
ε	emissivity	(-)
θ	cone half angle	(°)
ρ	reflectivity	(-)
τ	transmissivity	(-)
$\mathcal{F}_{i\text{-}j}$	exchange factor from surface i to j	(-)

Subscripts

1,2,3	surface number
d	diffuse component of reflectivity
e	exact analytical solution
s	specular component of reflectivity

Introduction

RadCAD™† is a Monte Carlo simulation designed for solving thermal radiation problems. RadCAD utilizes AutoCAD™‡ as the underlying CAD engine. Panczak and Ring discussed the integration and advantages of a CAD engine.[1,2] RadCAD allows analysts to read in existing CAD data bases, but also to create models interactively. Analysts have the choice of creating a model using AutoCAD surfaces or to use RadCAD's custom surfaces. Optical properties, orbit definition, and analysis parameters, are defined using pull down menus and dialog boxes. RadCAD has been developed for personal computers, which brings the capability of Monte Carlo simulation to low cost platforms.

As part of RadCAD's development process, it is necessary to validate results produced by RadCAD with exact analytical solutions and other radiation simulation tools. A comparison of form factors produced by RadCAD to exact solutions has already been performed.[3] This paper compares radiation exchange factors (or Radks) to exact solutions and results from TRASYS. Specular and diffuse exchange factors will be calculated for the internal surfaces of a cylinder and cone. Optical properties and dimensions

† RadCAD is a registered trademark of Cullimore and Ring Technologies.

‡ AutoCAD is a registered trademark of Autodesk.

were changed to create 98 cases. For each case the number of rays shot from each surface was increased from 1,000 to 100,000. RadCAD's results will be used to calculate an effective emissivity ($\bar{\varepsilon}$). An exact effective emissivity ($\bar{\varepsilon}_e$) for both a cone and cylinder was calculated by Lin and Sparrow[4]. Connolly and Lucas used this formulation to verify the specular exchange factors for TRASYS[5]. Comparisons to both TRASYS and the exact solution will be made.

In order to verify TRASYS's ray tracing algorithms, Connolly and Lucas used an adjunct plate system[5]. These authors compared TRASYS's results to both OPERA and NEVEADA results. Hering calculated the exact solution to adjunct plates[6]. Hering results were numerically integrated by Connolly and Lucas in order to make a comparison between TRASYS and OPERA , NEVADA and the exact solution. The current paper will compare RadCAD's results to the exact analytical solution, and results from TRASYS, OPERA and NEVADA. Optical properties and solar vector position will be changed to create 12 cases. The number of rays shot per surface will also be increased from 1,000 to 100,000 for each case.

Geometric Configurations

Three geometric configurations were considered to validate RadCAD's specular algorithms . Specular exchange factors were validated using the interior surfaces of a cone and cylinder. Specular solar fluxes were validated using the interior surfaces of a wedge. For all geometries, primary dimensions and optical properties were changed.

All surfaces are assumed to be opaque (τ=0). So, all radiant incident energy is either absorbed or reflected. Therefore, the sum of absorptivity (α) and reflectivity (ρ) is one, or

$$\alpha + \rho = 1 \qquad (1)$$

Also, Kirchoff's law applies to the surfaces. The emissivity and absorptivity are equal (ε=α). The reflectivity is defined in a typical manner as the sum of the specular (ρ_s) and diffuse (ρ_d) components, according to,

$$\rho = \rho_s + \rho_d \qquad (2)$$

The percent specularity of a surface is defined as the ratio of specular reflectivity to reflectivity, or

$$\frac{\rho_s}{\rho_s+\rho_d} \qquad (3)$$

Therefore, when a surface is 100% specular, the diffuse component of reflectivity is zero (ρ_d=0). From (3) it is concluded that the reflectivity is equal to the specular reflectivity ($\rho = \rho_s$).

The configurations and optical properties for each geometry will be discussed next.

Cone

The first geometric configuration considered consisted of a cone and a disk as shown in Figure 1. The cone has length L and a opening angle of 2θ. Surface 1 is defined as the cone and has an area, A_1. A disk is used to close out the geometry, and has an area A_2. Given L and θ the disk radius is easily calculated.

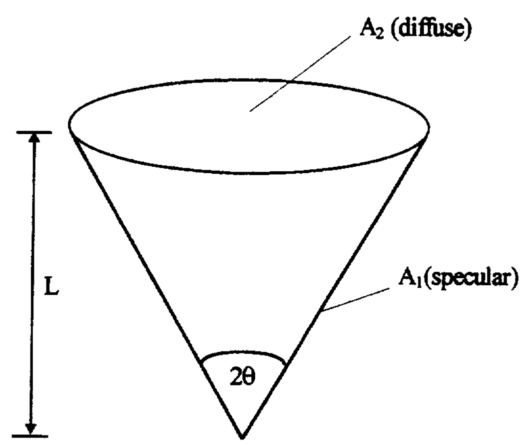

Figure 1 Cone Geometry

The disk radius, opening angle and optical properties were varied. The length remained fixed at a value of one (L=1) for all cases. The values for the half angle of the cone were: 10°, 20°, 30°, and 60°. Optical properties for surface 1 are given in Table 1. The disk had an emissivity of one and was considered diffuse for all cases. Surface 1 was considered to be 100% specular for all cases. As seen from Table 1, both ε and ρ (or ρ_s) varied from 0.1 to 0.9.

Table 1 Cone Optical Properties

ε = α	ρ=ρ_s		ε = α	ρ=ρ_s
0.1	0.9		0.5	0.5
0.2	0.8		0.7	0.3
0.3	0.7		0.9	0.1

Cylinder

The second geometric configuration consisted of a cylinder and two disks and is shown in Figure 2. As shown in this figure the cylinder had a radius R and length L. Surface 1 was defined as the cylinder, and has area, A_1. Surfaces 2 and 3 were defined as disks and had an area A_2 and A_3, respectively. Surfaces 1 and 2 were 100% specular for all specular cases. Surface 3 was diffuse and black for all cases.

Dimensions and optical properties of the cylinder were allowed to vary from case to case. Values for L/R were: 2, 4, 6, 8, and 10. Optical properties for surfaces 1 and 2 are defined in Table 2.

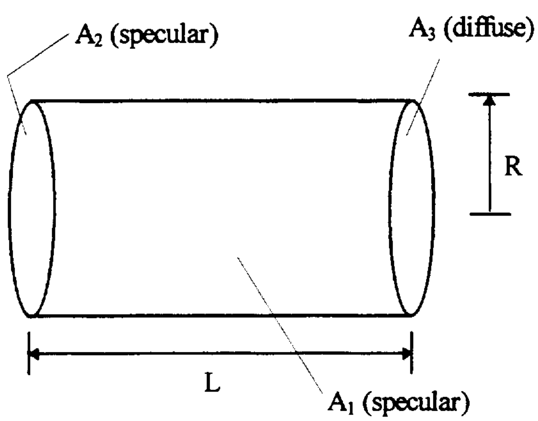

Figure 2 Cylinder Geometry

Table 2 Cylinder Optical Properties

$\varepsilon = \alpha$	$\rho=\rho_s$	$\varepsilon = \alpha$	$\rho=\rho_s$
0.1	0.9	0.7	0.3
0.3	0.7	0.9	0.1
0.5	0.5		

Wedge

A sketch of the wedge used to validate specular absorbed fluxes is shown in Figure 3. The nodal breakdown was chosen to "trap" rays in the wedge[5]. As shown in this figure two different solar angles were considered. Position 1 and 2 were 10° and 50°, respectively, from surface 1. The wedge was assumed to be 1 meter in length and 100% specular triangles were used at the ends.

Table 3 gives the optical properties used for the two solar positions. Values for ε were 0.1 and 0.5, and the wedge was assumed to be 0%, 50% and 100% specular. Values of ε, ρ_s and ρ_d are given in Table 3.

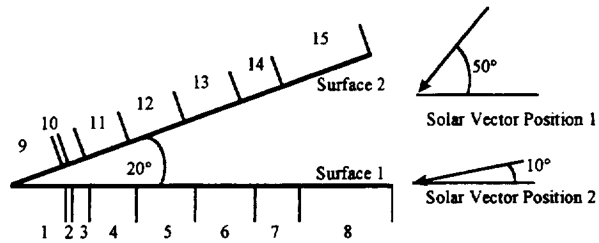

Nodal Break Down			
Surface 1		Surface 2	
Node	Location	Node	Location
1	0.1732	9	0.1732
2	0.1848	10	0.1848
3	0.2267	11	0.2267
4	0.3473	12	0.3473
5	0.5	13	0.5321
6	0.6527	14	0.8152
7	0.766	15	1.0
8	1.0		

Figure 3 Geometry for the Wedge

Table 3 Optical Properties for the Wedge

$\varepsilon = \alpha$	ρ_s	ρ_d
0.1	0.0	0.9
0.1	0.45	0.45
0.1	0.9	0.0
0.5	0.0	0.5
0.5	0.25	0.25
0.5	0.5	0.0

Exact Solutions

Exact solutions were found in the literature for all three geometries. Lin and Sparrow presented specular and diffuse exchange factors for the cone and cylinder geometries. Connolly and Lucas numerically integrated Hering's results for the wedge geometry.

Lin and Sparrow defined a radiating effectiveness ($\bar{\varepsilon}$) for cones and cylinders of various sizes and optical properties. The radiating effectiveness for a cavity is defined as,

$$\bar{\varepsilon} = \frac{Q_{e/ab}}{(Q_{e/ab})_b} \tag{4}$$

where, $Q_{e/ab}$ = radiant energy rate leaving the cavity

$(Q_{e/ab})_b$ = radiant energy rate leaving a black cavity.

Equation (4) is interpreted as the emissive performance of a non black cavity. A black cavity has the best performance. As the emissivity of the cavity approaches one, then $\bar{\varepsilon}$ approaches one.

Cone

The analytical results for radiating emissivities for both a specular ($\bar{\varepsilon}_{e,s}$)and diffuse ($\bar{\varepsilon}_{e,d}$) cone were taken from Reference 5, and are presented here in Table 4. Lin and Sparrow showed the specular solution and diffuse solution converged at a cone half angle of approximately 50°.

Table 4 Exact Results for Cone

$\varepsilon = 0.1, \rho = \rho_s = 0.9$			$\varepsilon = 0.5, \rho = \rho_s = 0.5$		
θ	$\bar{\varepsilon}_{e,s}$	$\bar{\varepsilon}_{e,d}$	θ	$\bar{\varepsilon}_{e,s}$	$\bar{\varepsilon}_{e,d}$
10	0.418	0.332	10	0.922	0.775
20	0.25	0.232	20	0.795	0.709
30	0.182	0.177	30	0.69	0.65
60	0.114	0.11	60	0.536	0.53
$\varepsilon = 0.2, \rho = \rho_s = 0.8$			$\varepsilon = 0.7, \rho = \rho_s = 0.3$		
θ	$\bar{\varepsilon}_{e,s}$	$\bar{\varepsilon}_{e,d}$	θ	$\bar{\varepsilon}_{e,s}$	$\bar{\varepsilon}_{e,d}$
10	0.655	0.5	10	0.973	0.882
20	0.445	0.398	20	0.914	0.845
30	0.33	0.323	30	0.85	0.814
60	0.222	0.22	60	0.727	0.72
$\varepsilon = 0.3, \rho = \rho_s = 0.7$			$\varepsilon = 0.9, \rho = \rho_s = 0.3$		
θ	$\bar{\varepsilon}_{e,s}$	$\bar{\varepsilon}_{e,d}$	θ	$\bar{\varepsilon}_{e,s}$	$\bar{\varepsilon}_{e,d}$
10	0.795	0.618	10	0.99	0.968
20	0.595	0.523	20	0.982	0.955
30	0.477	0.449	30	0.96	0.945
60	0.33	0.33	60	0.91	0.91

Cylinder

Analytical results for radiating emissivities for a specular and diffuse cylinder were taken from Reference 5, and are presented here in Table 5. For this geometry, Lin and Sparrow showed that the effective emissivity for both specular and diffuse optical properties did not change as a function of L/R for L/R>6.

Wedge

Hering solved the adjunct plate geometry in a general form. Connolly and Lucas numerically integrated Hering's results for solar position 2.

Table 6 shows these results. The solar flux has been assumed to be 1 W/m^2. This was done to facilitate viewing the results.

Table 5 Exact Results for Cylinder

$\varepsilon = 0.1, \rho = \rho_s = 0.9$			$\varepsilon = 0.7, \rho = \rho_s = 0.3$		
L/R	$\bar{\varepsilon}_{e,s}$	$\bar{\varepsilon}_{e,d}$	L/R	$\bar{\varepsilon}_{e,s}$	$\bar{\varepsilon}_{e,d}$
2	0.9919	0.977	2	0.7024	0.664
4	0.9975	0.977	4	0.8305	0.7136
6	0.9988	0.977	6	0.8909	0.718
8	0.9993	0.977	8	0.9244	0.718
10	0.9996	0.977	10	0.9448	0.718
$\varepsilon = 0.3, \rho = \rho_s = 0.7$			$\varepsilon = 0.9, \rho = \rho_s = 0.1$		
L/R	$\bar{\varepsilon}_{e,s}$	$\bar{\varepsilon}_{e,d}$	L/R	$\bar{\varepsilon}_{e,s}$	$\bar{\varepsilon}_{e,d}$
2	0.9547	0.909	2	0.3486	0.3486
4	0.9833	0.918	4	0.4931	0.45
6	0.9916	0.918	6	0.5912	0.477
8	0.995	0.918	8	0.6624	0.489
10	0.9967	0.918	10	0.7161	0.495
$\varepsilon = 0.5, \rho = \rho_s = 0.5$					
L/R	$\bar{\varepsilon}_{e,s}$	$\bar{\varepsilon}_{e,d}$			
2	0.8717	0.809			
4	0.9422	0.836			
6	0.9677	0.836			
8	0.9797	0.836			
10	0.9861	0.836			

Table 6 Exact Solution Results for Wedge

	Flux [W/m^2]					
	α=0.1			α=0.5		
Node	ρ_s/ρ=0.0	ρ_s/ρ=0.5	ρ_s/ρ=1.0	ρ_s/ρ=0.0	ρ_s/ρ=0.5	ρ_s/ρ=1.0
1	0.02025	0.03535	0.06688	0.02899	0.04532	0.07283
2	0.00124	0.00192	0.00372	0.00192	0.00291	0.00452
3	0.00437	0.00613	0.00823	0.00691	0.01003	0.01323
4	0.01167	0.01299	0.01131	0.01963	0.02466	0.02582
5	0.01300	0.00950	0.00379	0.02410	0.01948	0.01331
6	0.01107	0.00760	0.00379	0.02300	0.01835	0.01331
7	0.00695	0.00482	0.00281	0.01606	0.01304	0.00988
8	0.01086	0.00808	0.00581	0.02944	0.02508	0.02040
9	0.02025	0.03535	0.06688	0.02899	0.04532	0.07283
10	0.00124	0.00192	0.00372	0.00192	0.00291	0.00452
11	0.00437	0.00613	0.00823	0.00691	0.01003	0.01323
12	0.01167	0.01299	0.01131	0.01963	0.02466	0.02582
13	0.01548	0.01118	0.00459	0.02905	0.02338	0.01611
14	0.01822	0.01255	0.00703	0.04088	0.03297	0.02468
15	0.00819	0.00619	0.00459	0.02278	0.01958	0.01611
sum	0.15883	0.1727	0.21269	0.30021	0.31772	0.3466

Computer Simulation Results

The aforementioned geometries have been analyzed using various radiation computer software tools. TRASYS was used to calculate specular radiating effectiveness for both the cone and cylinder[5]. TRASYS, OPERA, and NEVADA have been used to analyze the wedge geometry[5].

In order to calculate the radiating effectiveness exchange factors ($\mathcal{F}_{i-j}$) were needed for the cone and cylinder. An exchange factor between surface i and j is defined as the fraction of energy that leaves i and is absorbed by j by all possible paths, including specular and diffuse reflections. The product of area and exchange factor is often referred to as a Radk.

Cone

Using equation (4) the effective emissivity for a cone is

$$\bar{\varepsilon} = \mathcal{F}_{1-2} / \sin\theta \qquad (5)$$

where, $\mathcal{F}_{1-2}$ is the exchange factor between the cone and disk.

Table 7 Specular Effective Emissivity for the Cone from TRASYS and RadCAD

Optical Properties	θ	Effective Emissivity TRASYS	RadCAD Varying N_r 1000	10000	100000
ε=0.1 ρ=ρs=0.9	10	0.4238	0.4253	0.4217	0.4230
	20	0.2526	0.2527	0.2539	0.2540
	30	0.183	0.1847	0.1842	0.1843
	60	0.1129	0.1138	0.1135	0.1136
ε=0.2 ρ=ρs=0.8	10	0.6577	0.6612	0.6563	0.6574
	20	0.4444	0.4448	0.4467	0.4474
	30	0.3398	0.3426	0.3412	0.3422
	60	0.2224	0.2240	0.2242	0.2238
ε=0.3 ρ=ρs=0.7	10	0.7923	0.7864	0.7922	0.7923
	20	0.5903	0.6025	0.5949	0.5963
	30	0.4742	0.4773	0.4769	0.4777
	60	0.3287	0.3300	0.3310	0.3309
ε=0.5 ρ=ρs=0.5	10	0.9233	0.9213	0.9277	0.9212
	20	0.7856	0.8001	0.7966	0.7983
	30	0.6867	0.6890	0.6971	0.6940
	60	0.532	0.5365	0.5356	0.5353
ε=0.3 ρ=ρs=0.7	10	0.9749	0.9811	0.9681	0.9708
	20	0.898	0.9177	0.9127	0.9153
	30	0.839	0.8487	0.8496	0.8500
	60	0.7238	0.7340	0.7287	0.7301
ε=0.9 ρ=ρs=0.1	10	0.9959	1.0174	0.9924	0.9904
	20	0.9668	0.9794	0.9801	0.9812
	30	0.9454	0.9573	0.9577	0.9603
	60	0.9046	0.9114	0.9076	0.9125

The specular effective emissivities for the cone geometry were calculated using Radks produced by RadCAD. The cone half angle was varied as discussed above, and the optical properties varied according to Table 1. The number of rays shot per surfaces (N_r) was also allowed to vary. TRASYS has also been used to generate Radks and effective emissivities [5]. Both the RadCAD and TRASYS results are given in Table 7.

Diffuse effective emissivities were generated based upon diffuse Radks produced by RadCAD. These results are given in Table 8 for varying number of rays shot per surface. For these results the reflectivity was equal to the diffuse component ($\rho=\rho_d$).

Table 8 Diffuse Effective Emissivity for the Cone from RadCAD

Optical Properties	θ	Effective Emissivity RadCAD Varying N_r 1000	10000	100000
ε=0.1 ρ=ρd=0.9	10	0.3259	0.3344	0.3325
	20	0.2354	0.2335	0.2340
	30	0.1785	0.1791	0.1789
	60	0.1137	0.1136	0.1137
ε=0.2 ρ=ρd=0.8	10	0.4988	0.5000	0.4987
	20	0.3987	0.3970	0.3974
	30	0.3219	0.3258	0.3251
	60	0.2232	0.2240	0.2238
ε=0.3 ρ=ρd=0.7	10	0.6199	0.6140	0.6127
	20	0.5267	0.5205	0.5224
	30	0.4434	0.4525	0.4493
	60	0.3352	0.3301	0.3306
ε=0.5 ρ=ρd=0.5	10	0.7540	0.7684	0.7721
	20	0.7091	0.7099	0.7098
	30	0.6559	0.6485	0.6502
	60	0.5390	0.5354	0.5350
ε=0.3 ρ=ρd=0.7	10	0.8862	0.8789	0.8790
	20	0.8351	0.8459	0.8470
	30	0.8080	0.8105	0.8090
	60	0.7309	0.7300	0.7285
ε=0.9 ρ=ρd=0.1	10	0.9710	0.9633	0.9606
	20	0.9519	0.9501	0.9560
	30	0.9445	0.9424	0.9403
	60	0.9147	0.9123	0.9113

Cylinder

Using equation (4) the effective emissivity for a cylinder is

$$\bar{\varepsilon} = 2L\mathcal{F}_{1-3}/R + \mathcal{F}_{2-3} \qquad (6)$$

where, $\mathcal{F}_{1-2}$ is the exchange factor between the cylinder and the diffuse disk.

$\mathcal{F}_{2\text{-}3}$ is the exchange factor between the specular disk and the diffuse disk.

The specular effective emissivities for the cylinder geometry were calculated using Radks produced by RadCAD. The length to radius ratio was varied as discussed above, and the optical properties varied according to Table 1. The number of rays shot per surfaces was also allowed to vary. TRASYS was also was used to generate Radks and effective emissivities were then calculated[5]. Both the RadCAD and TRASYS results are given in Table 9.

Diffuse effective emissivities were generated based upon diffuse Radks produced by RadCAD. These results are given in Table 10 for varying number of rays shot per surface. For these results the reflectivity was equal to the diffuse component ($\rho=\rho_d$).

Table 9 Specular Effective Emissivity for the Cylinder from TRASY and RadCAD

Optical Properties	L/R	Effective Emissivity			
		TRASYS	RadCAD Varying N_r 1000	10000	100000
ε=0.1 $\rho=\rho_s$=0.9	2	0.336	0.3513	0.3483	0.3486
	4	0.475	0.4931	0.4965	0.4928
	6	0.5611	0.6021	0.5895	0.5908
	8	0.6127	0.6566	0.6603	0.6613
	10	0.6456	0.7189	0.7192	0.7158
ε=0.3 $\rho=\rho_s$=0.7	2	0.6677	0.7069	0.7003	0.7027
	4	0.7931	0.8258	0.8277	0.8318
	6	0.8318	0.8857	0.8888	0.8905
	8	0.8609	0.9179	0.9253	0.9253
	10	0.8483	0.9524	0.9468	0.9443
ε=0.5 $\rho=\rho_s$=0.5	2	0.8419	0.8728	0.8750	0.8704
	4	0.9227	0.9461	0.9477	0.9407
	6	0.9246	0.9696	0.9682	0.9695
	8	0.9362	0.9873	0.9813	0.9813
	10	0.9221	0.9875	0.9831	0.9855
ε=0.7 $\rho=\rho_s$=0.3	2	0.9341	0.9559	0.9581	0.9549
	4	0.9917	0.9969	0.9836	0.9836
	6	0.9644	0.9925	0.9911	0.9927
	8	0.9682	0.9823	0.9930	0.9951
	10	0.9589	1.0083	0.9956	0.9967
ε=0.9 $\rho=\rho_s$=0.1	2	0.9797	1.0053	0.9917	0.9921
	4	1.0002	0.9769	0.9986	0.9958
	6	0.9855	1.0029	1.0004	0.9980
	8	0.9879	0.9945	0.9990	0.9992
	10	0.984	0.9943	1.0006	0.9986

Table 10 Diffuse Effective Emissivity for the Cylinder from RadCAD

Optical Properties	L/R	Effective Emissivity RadCAD Varying N_r 1000	10000	100000
ε=0.1 $\rho=\rho_d$=0.9	2	0.3503	0.3468	0.3474
	4	0.4472	0.4457	0.4463
	6	0.4860	0.4812	0.4788
	8	0.4810	0.4956	0.4920
	10	0.4959	0.4896	0.4976
ε=0.3 $\rho=\rho_d$=0.7	2	0.6666	0.6596	0.6574
	4	0.7086	0.7168	0.7097
	6	0.7152	0.7159	0.7192
	8	0.7166	0.7253	0.7194
	10	0.7128	0.7195	0.7215
ε=0.5 $\rho=\rho_d$=0.5	2	0.8119	0.8045	0.8090
	4	0.8482	0.8306	0.8307
	6	0.8432	0.8456	0.8370
	8	0.8349	0.8383	0.8356
	10	0.8454	0.8364	0.8371
ε=0.7 $\rho=\rho_d$=0.3	2	0.9117	0.9045	0.9033
	4	0.9098	0.9108	0.9144
	6	0.9245	0.9180	0.9139
	8	0.9193	0.9112	0.9156
	10	0.9136	0.9153	0.9144
ε=0.9 $\rho=\rho_d$=0.1	2	0.9740	0.9780	0.9707
	4	0.9673	0.9793	0.9743
	6	0.9734	0.9750	0.9751
	8	0.9821	0.9744	0.9766
	10	0.9773	0.9763	0.9755

Wedge

RadCAD was used to calculate absorbed fluxes for the wedge using solar position 1 and 2. Results for position 1 are given in Table 11 and Table 12. The first table gives the absorbed fluxes of α=0.1 and varying values of reflectivity. The second table gives similar information except for α=0.5. Due to the large amount of data only this solar angle will be presented here. This angle was chosen since exact solutions were given in Table 6. Results for both solar angles for OPERA, NEVADA and TRASYS can be found in Reference 5.

A comparison of effective emissivities and absorbed fluxes for all geometries will be presented next.

Table 11 Absorbed Fluxes from RadCAD ε=0.1

	Flux [W/m^2]								
	α=0.1 ρ_s/ρ=0.0			α=0.1 ρ_s/ρ=0.5			α=0.1 ρ_s/ρ=1.0		
Node	1000	10,000	100,000	1000	10,000	100,000	1000	10,000	100,000
1	0.02074	0.02061	0.02067	0.03620	0.03585	0.03575	0.06701	0.06687	0.06686
2	0.00128	0.00125	0.00125	0.00196	0.00190	0.00193	0.00362	0.00372	0.00376
3	0.00446	0.00440	0.00441	0.00618	0.00618	0.00616	0.00815	0.00825	0.00824
4	0.01201	0.01174	0.01177	0.01279	0.01315	0.01312	0.01138	0.01132	0.01130
5	0.01298	0.01318	0.01313	0.00964	0.00966	0.00965	0.00379	0.00379	0.00379
6	0.01106	0.01110	0.01115	0.00769	0.00767	0.00764	0.00379	0.00379	0.00379
7	0.00701	0.00699	0.00701	0.00487	0.00484	0.00485	0.00281	0.00281	0.00281
8	0.01114	0.01092	0.01096	0.00807	0.00808	0.00813	0.00581	0.00581	0.00581
9	0.02080	0.02057	0.02067	0.03591	0.03588	0.03576	0.06687	0.06683	0.06687
10	0.00121	0.00127	0.00126	0.00197	0.00192	0.00194	0.00375	0.00380	0.00375
11	0.00440	0.00444	0.00441	0.00618	0.00615	0.00617	0.00823	0.00823	0.00823
12	0.01183	0.01177	0.01178	0.01311	0.01309	0.01312	0.01131	0.01131	0.01131
13	0.01555	0.01563	0.01562	0.01142	0.01140	0.01138	0.00459	0.00459	0.00459
14	0.01842	0.01826	0.01836	0.01250	0.01264	0.01265	0.00703	0.00703	0.00703
15	0.00833	0.00824	0.00828	0.00635	0.00620	0.00622	0.00459	0.00459	0.00459
sum	0.16122	0.16037	0.16073	0.17484	0.17461	0.17447	0.21273	0.21274	0.21273

Table 12 Absorbed Fluxes from RadCAD ε=0.5

	Flux [W/m^2]								
	α=0.5 ρ_s/ρ=0.0			α=0.5 ρ_s/ρ=0.5			α=0.5 ρ_s/ρ=1.0		
Node	1000	10,000	100,000	1000	10,000	100,000	1000	10,000	100,000
1	0.02877	0.02904	0.02894	0.04521	0.04529	0.04524	0.07298	0.07287	0.07283
2	0.00204	0.00189	0.00192	0.00300	0.00290	0.00292	0.00441	0.00451	0.00452
3	0.00695	0.00683	0.00691	0.01025	0.00997	0.01006	0.01334	0.01321	0.01321
4	0.01957	0.01951	0.01957	0.02446	0.02471	0.02467	0.02569	0.02582	0.02585
5	0.02435	0.02416	0.02410	0.01961	0.01955	0.01958	0.01331	0.01331	0.01331
6	0.02258	0.02316	0.02299	0.01829	0.01848	0.01836	0.01331	0.01331	0.01331
7	0.01605	0.01611	0.01611	0.01298	0.01290	0.01304	0.00988	0.00988	0.00988
8	0.02967	0.02941	0.02950	0.02485	0.02506	0.02507	0.02040	0.02040	0.02040
9	0.02892	0.02900	0.02894	0.04545	0.04522	0.04526	0.07291	0.07285	0.07282
10	0.00186	0.00190	0.00192	0.00284	0.00293	0.00292	0.00452	0.00450	0.00454
11	0.00689	0.00691	0.00689	0.01007	0.01003	0.01006	0.01317	0.01324	0.01324
12	0.01972	0.01951	0.01958	0.02441	0.02477	0.02466	0.02582	0.02582	0.02582
13	0.02906	0.02912	0.02909	0.02364	0.02344	0.02348	0.01611	0.01611	0.01611
14	0.04045	0.04091	0.04076	0.03277	0.03290	0.03297	0.02468	0.02468	0.02468
15	0.02298	0.02275	0.02281	0.01976	0.01954	0.01959	0.01611	0.01611	0.01611
sum	0.29986	0.30021	0.30003	0.31759	0.31769	0.31788	0.34664	0.34662	0.34663

Comparison of Results

A comparison between RadCAD and the analytical solution and results from other radiation simulation software will be presented next. For all comparisons the percent error will be defined as,

$$E = (1 - \frac{R_A}{R_S}) \times 100 \quad (7)$$

where, R_A is the analytical result whether radiating effectiveness or flux and

R_S is the simulation tool result whether radiating effectiveness or flux.

The percent error will be both positive and negative in value. A positive value implies that the simulation tool over predicted the parameter in question. A negative value means the simulation tool under predicted.

Cone

Using equation (7), Table 4 and Table 7 comparisons between the analytical solution and calculated specular radiating effectiveness using both RadCAD and TRASYS results were made. These comparisons are shown in Figure 4 through Figure 9 where the percent errors as a function of half cone angle for the cone geometry with specular optical properties are presented. In each of the figures, the TRASYS results are presented first, followed by the RadCAD results. The number of rays shot as shown in the figures varied from 1,000 to 100,000, therefore there are three percent errors based upon RadCAD results for every TRASYS.

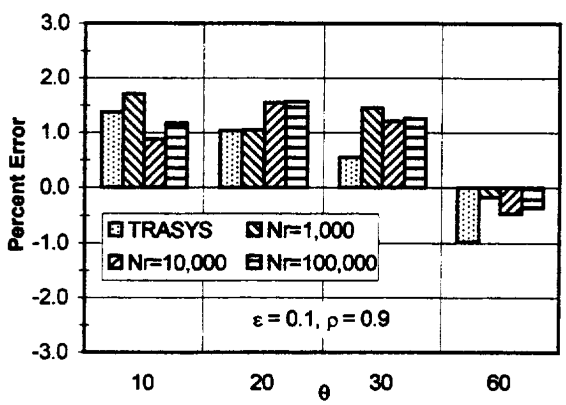

Figure 4 Cone Percent Error for Specular Radiating Effectiveness ε=0.1

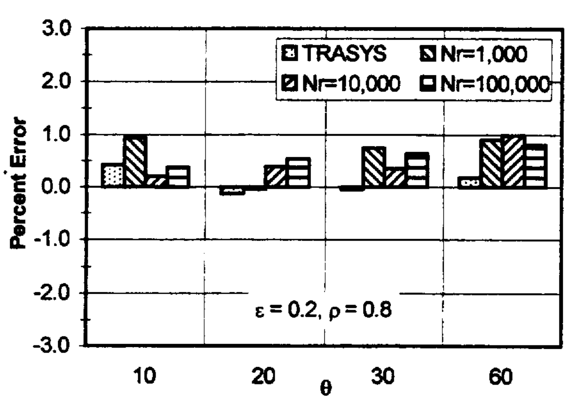

Figure 5 Cone Percent Error for Specular Radiating Effectiveness ε=0.2

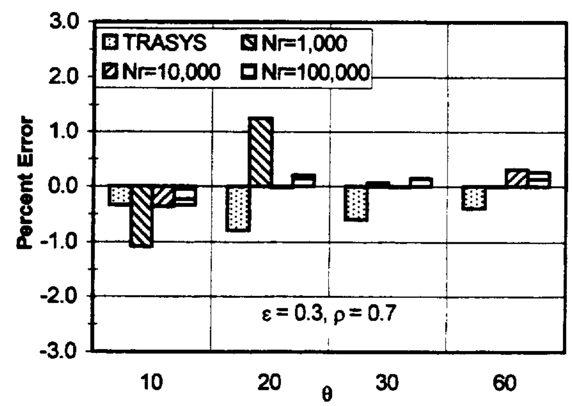

Figure 6 Cone Percent Error for Specular Radiating Effectiveness ε=0.3

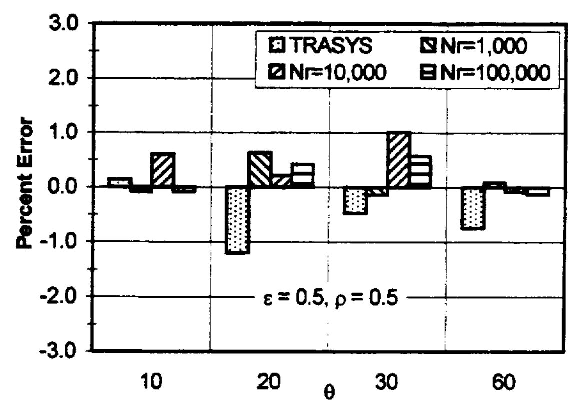

Figure 7 Cone Percent Error for Specular Radiating Effectiveness ε=0.5

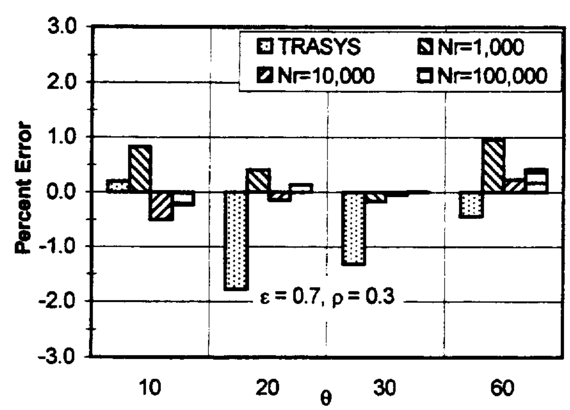

Figure 8 Cone Percent Error for Specular Radiating Effectiveness ε=0.7

Using equation (7), Table 4, and Table 8 comparisons between the analytical solution and calculated diffuse radiating effectiveness using RadCAD were made. These comparisons are shown in Table 13. The percent errors are listed for varying half cone angle for the cone geometry with diffuse optical properties. The number of rays shot varied from 1,000 to 100,000.

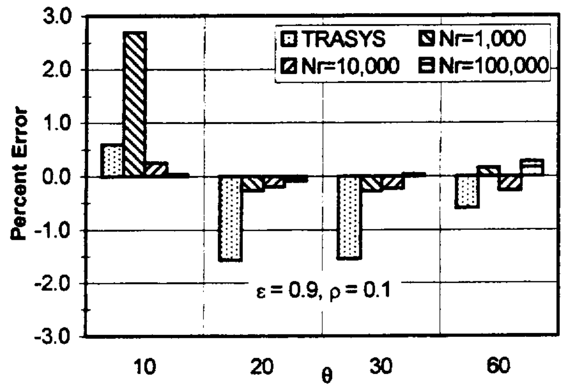

Figure 9 Cone Percent Error for Specular Radiating Effectiveness ε=0.9

Table 13 Cone Percent Error for Diffuse Radiating Effectiveness

Optical Properties	θ	Percent Error RadCAD Varying N_r 1000	10000	100000
ε=0.1 $\rho=\rho_d=0.9$	10	-1.83	0.72	0.14
	20	1.45	0.63	0.88
	30	0.86	1.17	1.05
	60	-0.24	-0.31	-0.29
ε=0.2 $\rho=\rho_d=0.8$	10	-0.24	-0.00	-0.25
	20	0.18	-0.26	-0.16
	30	-0.34	0.87	0.65
	60	0.53	0.80	1.72
ε=0.3 $\rho=\rho_d=0.7$	10	0.30	-0.65	-0.86
	20	0.71	-0.48	-0.11
	30	-1.24	0.78	0.06
	60	1.58	0.03	0.20
ε=0.5 $\rho=\rho_d=0.5$	10	-2.71	-0.85	-0.38
	20	0.01	0.13	0.12
	30	0.91	-0.23	0.04
	60	0.56	-0.12	-0.18
ε=0.7 $\rho=\rho_d=0.3$	10	0.47	-0.36	-0.34
	20	-1.17	0.10	0.24
	30	-0.73	-0.43	-0.61
	60	0.56	0.42	0.20
ε=0.9 $\rho=\rho_d=0.1$	10	0.31	-0.48	-0.76
	20	-0.32	-0.52	0.10
	30	-0.05	-0.27	-0.50
	60	0.51	0.26	0.14

Cylinder

Comparisons between the analytical solution and calculated specular radiating effectiveness using both RadCAD and TRASYS results were made. The results of these comparisons are shown in Figure 10 through Figure 14. Where the percent errors as a function of the length to radius ratio for the cylinder geometry with specular optical properties are presented. In each of the figures, the TRASYS results are presented first, followed the RadCAD results. The number of rays shot as shown in the figures varied from 1,000 to 100,000, therefore there are three percent errors based upon RadCAD results for every TRASYS.

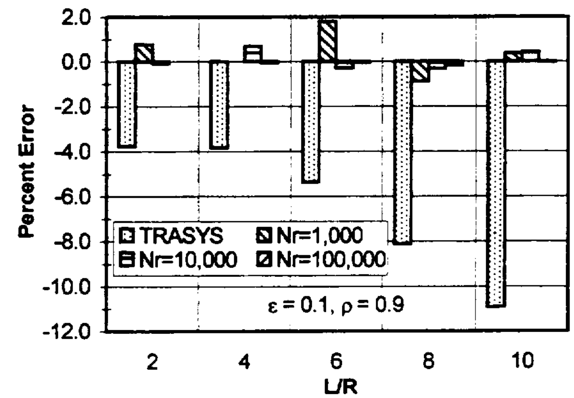

Figure 10 Cylinder Percent Error for Specular Radiating Effectiveness ε=0.1

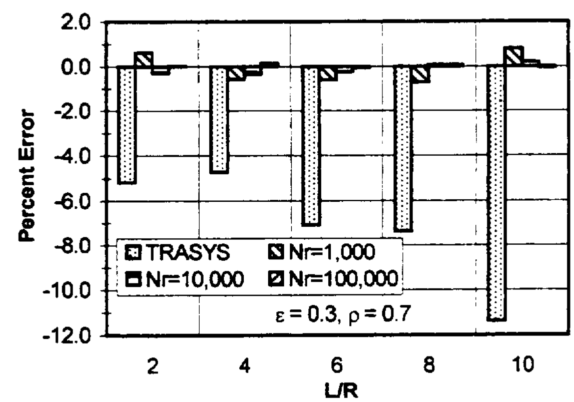

Figure 11 Cylinder Percent Error for Specular Radiating Effectiveness ε=0.3

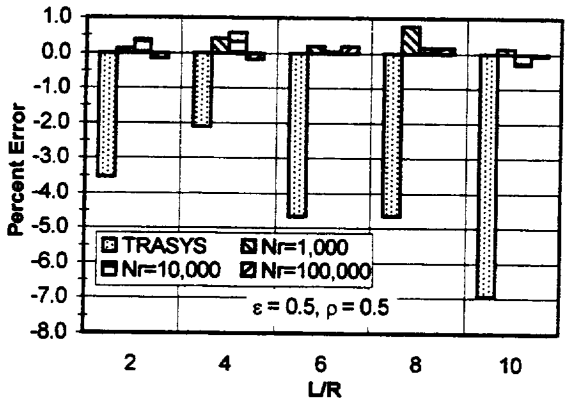

Figure 12 Cylinder Percent Error for Specular Radiating Effectiveness ε=0.5

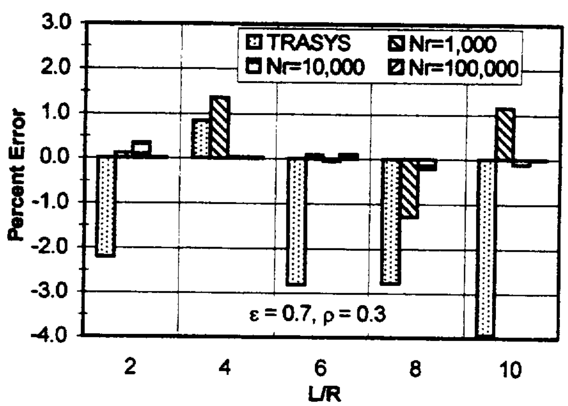

Figure 13 Cylinder Percent Error for Specular Radiating Effectiveness ε=0.7

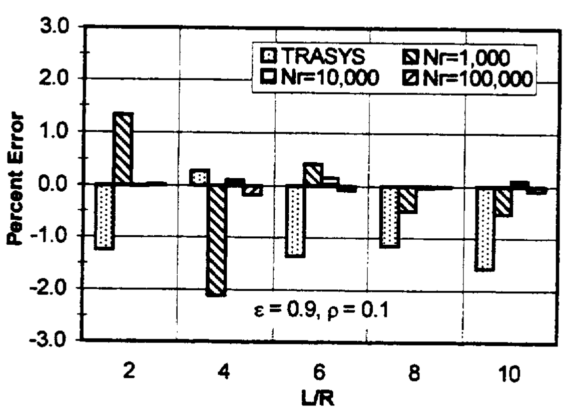

Figure 14 Cylinder Percent Error for Specular Radiating Effectiveness ε=0.9

Comparisons between the analytical solution and calculated diffuse radiating effectiveness using RadCAD were made. These comparisons are shown in Table 14 where the percent errors are listed for varying length to radius ratios for the cylinder geometry with diffuse optical properties. These comparisons were based on equation (7), Table 5, and Table 10. The number of rays shot varied from 1,000 to 100,000.

Table 14 Cylinder Percent Error for Diffuse Radiating Effectiveness

Optical Properties	L/R	Percent Error RadCAD Varying N_r 1000	10000	100000
ε=0.1 ρ=ρ_d=0.9	2	0.490	-0.532	-0.348
	4	-0.619	-0.959	-0.837
	6	1.843	0.882	0.369
	8	-1.655	1.330	0.612
	10	0.188	-1.100	0.513
ε=0.3 ρ=ρ_d=0.7	2	0.387	-0.663	-0.999
	4	-0.712	0.441	-0.556
	6	-0.392	-0.288	0.167
	8	-0.201	1.011	0.194
	10	-0.725	0.215	0.484
ε=0.5 ρ=ρ_d=0.5	2	0.356	-0.562	0.000
	4	1.443	-0.653	-0.644
	6	0.850	1.137	0.115
	8	-0.134	0.277	-0.053
	10	1.113	0.050	0.133
ε=0.7 ρ=ρ_d=0.3	2	0.293	-0.495	-0.636
	4	-0.896	-0.788	-0.395
	6	0.705	0.003	-0.449
	8	0.137	-0.744	-0.267
	10	-0.482	-0.298	-0.391
ε=0.9 ρ=ρ_d=0.1	2	-0.311	0.102	-0.645
	4	-0.998	0.233	-0.280
	6	-0.365	-0.209	-0.200
	8	0.519	-0.267	-0.042
	10	0.031	-0.072	-0.154

Wedge

The percent error for the absorbed fluxes for solar position 1 as calculated by (7) are shown in Figure 15 through Figure 20. These figures give a comparison for RadCAD, OPERA, NEVADA, and TRASYS to the exact solution. The absorbed flux as calculated by each radiation simulation tool for solar position 2 is shown in Figure 21 through Figure 26. A comparison is made for each node. These figures are presented after the references.

Discussion

A comparison of RadCAD results to both exact analytical solutions and other radiation simulation programs has been made. A discussion of the results will follow.

Cone

Overall the agreement between RadCAD and the analytical solution is quite good. The error from results produced by RadCAD ranged from -2.8% to 1.1% for a 1,000 rays. When 100,000 rays were shot the minimum and maximum error reduced to -1.6% and 0.36% respectively. While the minimum and maximum error produced by TRASYS was -1.39% and 1.8%. The values for the exact solution were taken from Figure 4 of Reference 4. There is some inherent uncertainty in reading this figure. The error for the diffuse results varied from -1.6% to 2.7% for 1,000 rays and -1.0% to 0.9% for 100,000 rays.

Cylinder

Overall the agreement between RadCAD and the analytical solution is quite good for the cylinder geometry. The error from results produced by RadCAD ranged from -2.0% to 2% for a 1,000 rays. When 100,000 rays were shot the minimum and maximum error reduced to -0.2% and 0.2% respectively. The TRASYS results were not quite as good the minimum and maximum error produced by TRASYS was -0.9% and 10.0%. The values for the exact solution were taken from equation (47) of Reference 4 and were evaluated by Reference 5. So, there is not the same uncertainty that existed in the cone results. The error for the diffuse results varied from -1.6% to 1.9% for 1,000 rays and -1.0% to 1.0% for 100,000 rays.

Wedge

The comparison for the absorbed fluxes was quite good. For solar position 1 RadCAD results differed by a maximum of -3.4% from the exact analytical solution for all nodes and optical properties considered. As can be seen by the data presented for the solar position 2, RadCAD results show good agreement with other radiation simulation software. This solar position offered an excellent case to verify RadCAD's ray tracing algorithms. In this case some nodes will not receive any of the incoming flux.

Conclusion

Both RadCAD's exchange factors and absorbed fluxes have been compared to exact analytical solutions and other existing radiation software tools. The agreement is good for all cases considered. RadCAD's specular capabilities can be used with confidence.

Acknowledgments

RadCAD development has been funded by the NASA Marshall Space Flight Center, with Mr. Bill Till serving as technical monitor.

References

1. Panczak, T. and Ring, S., "RadCAD: Integrating Radiation Analysis with Modern CAD Systems," SAE paper 961375, 26th ICES Conference, July 1996.

2. Panczak, T. and Ring, S., "RadCAD: Next Generation Thermal Radiation", SAE paper 972241, 27th ICES Conference, July 1997.

3. Lucas, S., "RadCAD: Validation of a New Thermal Radiation Analyzer," SAE paper 972242, 27th ICES Conference, July 1997.

4. Lin, S. H. and Sparrow, E. M., "Radiant Interchange Among Curved Specularly Reflecting Surfaces --- Application to Cylindrical and Conical Cavities," Journal of Heat Transfer, Transaction of ASME, May 1965, pp. 299-307.

5. Connolly, M. and Lucas, S., "Ray Tracing Capabilities in TRASYS," Interoffice Memorandum Martin Marietta, November 5, 1990.

6. Hering, R. G., "Radiative Heat Exchange and Equilibrium Surface Temperature in a Space Environment," Journal of Spacecraft, Vol. 5, January 1968, pp. 47-55.

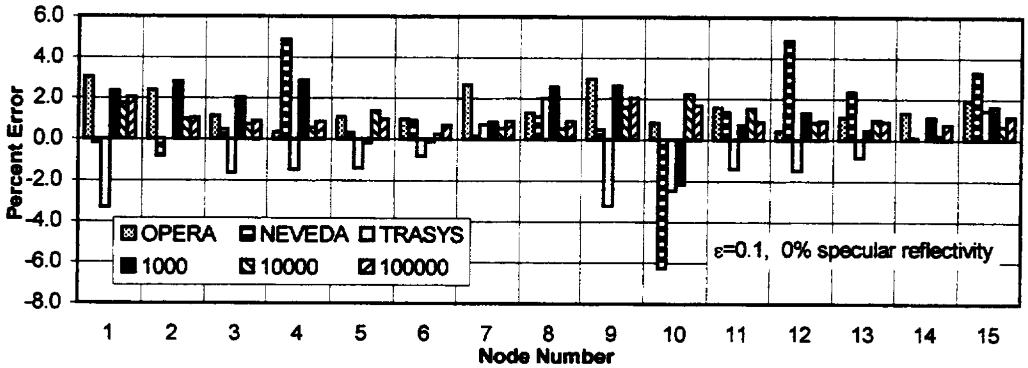

Figure 15 Wedge Percent Error for ε=0.1 and 0% Specular Reflectivity Solar Position 1

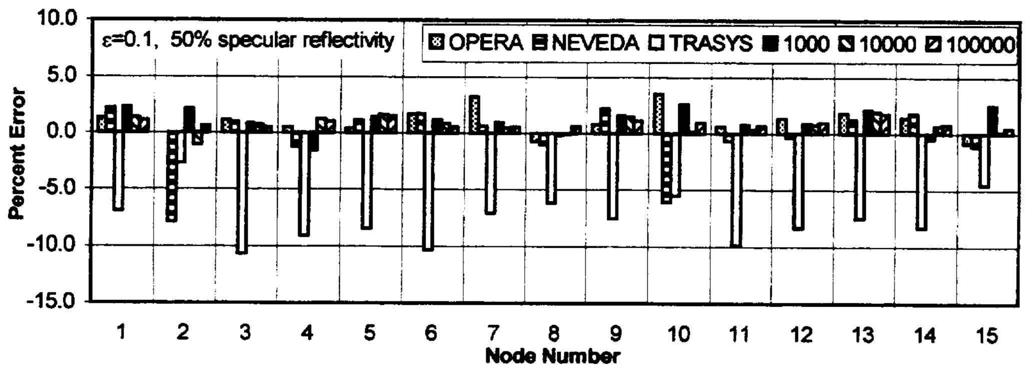

Figure 16 Wedge Percent Error for ε=0.1 and 50% Specular Reflectivity Solar Position 1

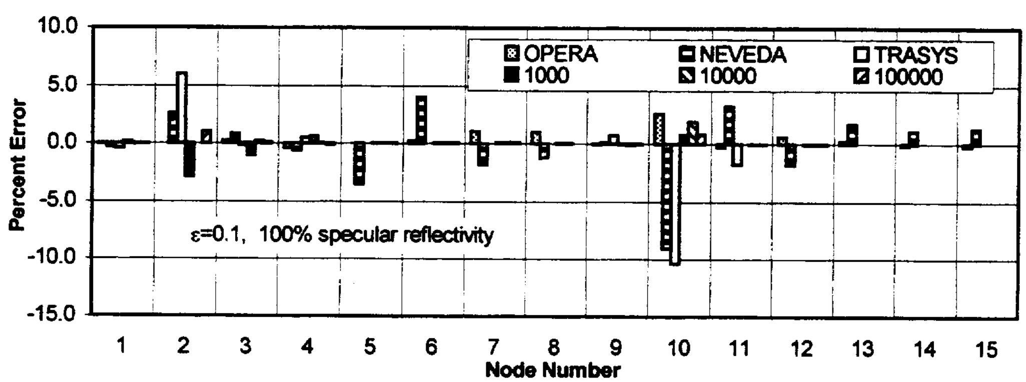

Figure 17 Wedge Percent Error for ε=0.1 and 100% Specular Reflectivity Solar Position 1

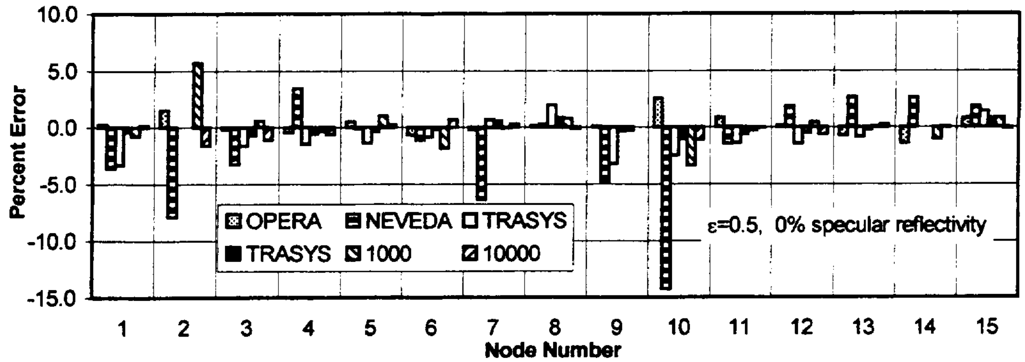

Figure 18 Wedge Percent Error for ε=0.5 and 0% Specular Reflectivity Solar Position 1

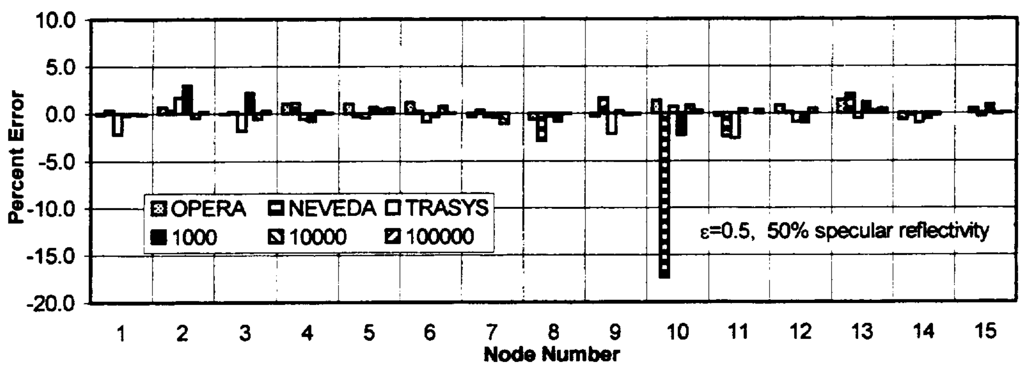

Figure 19 Wedge Percent Error for ε=0.5 and 50% Specular Reflectivity Solar Position 1

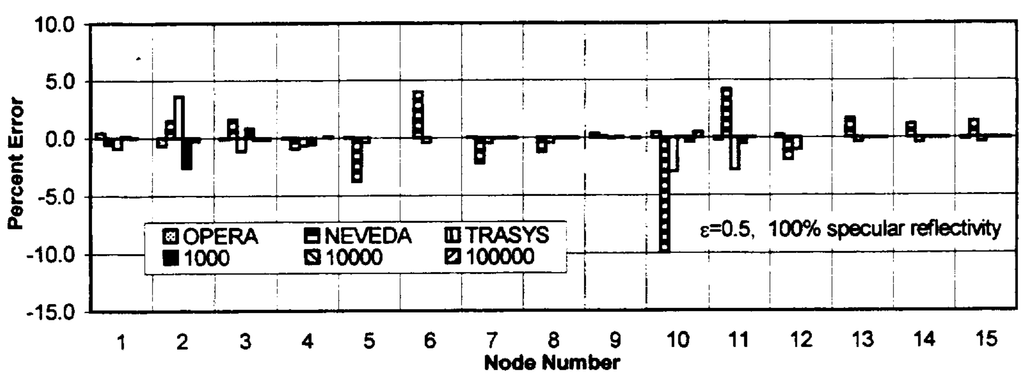

Figure 20 Wedge Percent Error for ε=0.5 and 100% Specular Reflectivity Solar Position 1

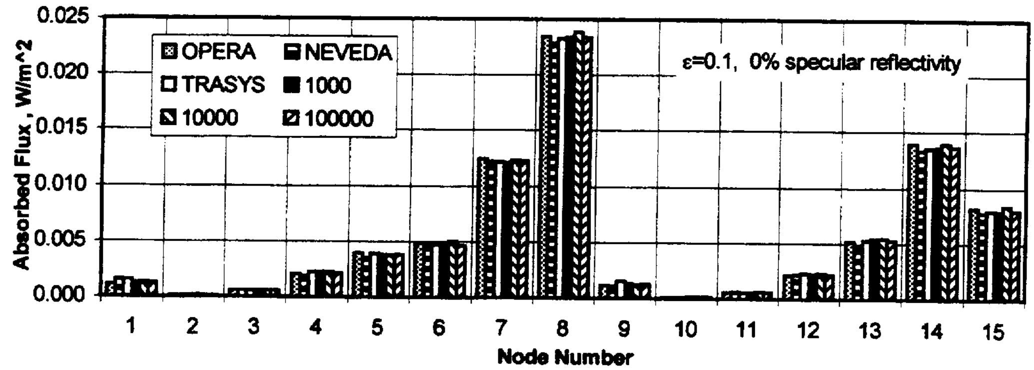

Figure 21 Wedge Absorbed Flux for ε=0.1 and 0% Specular Reflectivity Solar Position 2

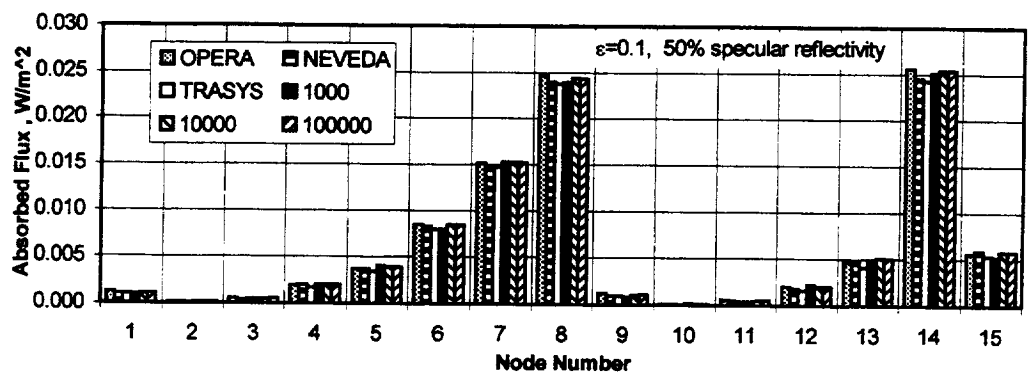

Figure 22 Wedge Absorbed Flux for ε=0.1 and 50% Specular Reflectivity Solar Position 2

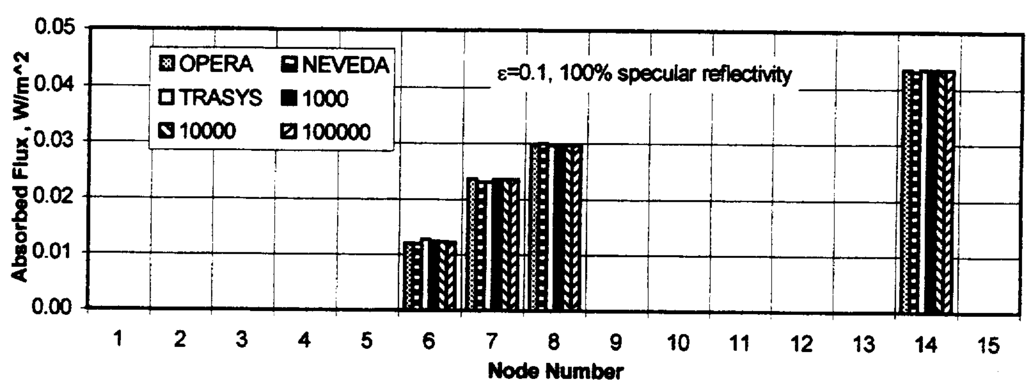

Figure 23 Wedge Absorbed Flux for ε=0.1 and 100% Specular Reflectivity Solar Position 2

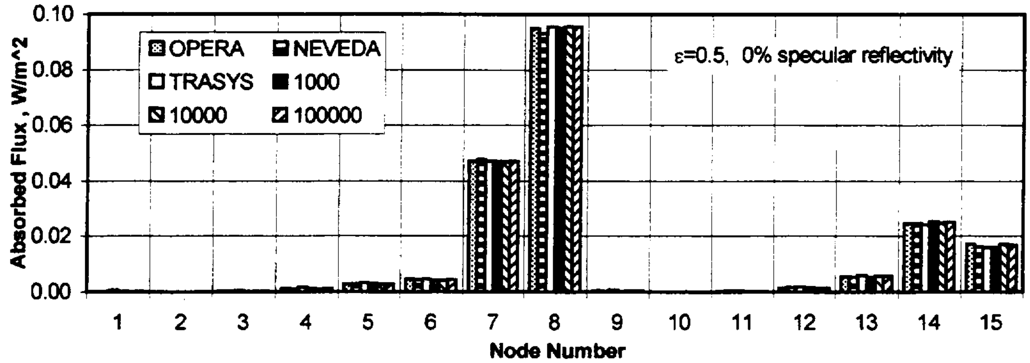

Figure 24 Wedge Absorbed Flux for ε=0.5 and 0% Specular Reflectivity Solar Position 2

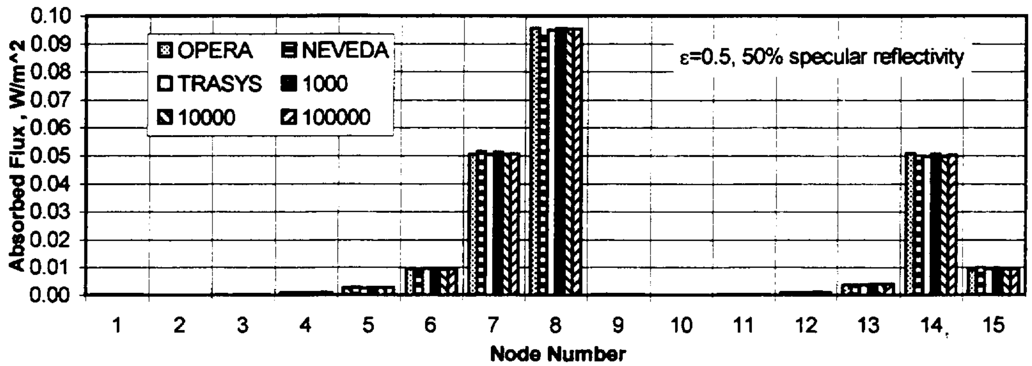

Figure 25 Wedge Absorbed Flux for ε=0.5 and 50% Specular Reflectivity Solar Position 2

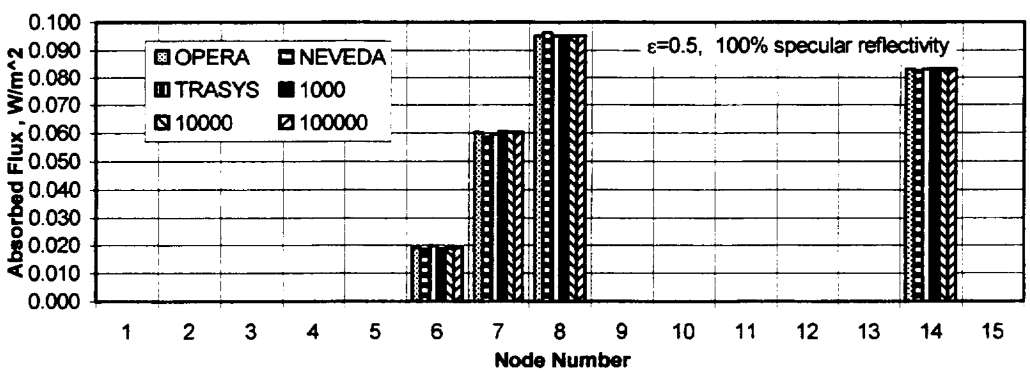

Figure 26 Wedge Absorbed Flux for ε=0.5 and 100% Specular Reflectivity Solar Position 2